Pergamon

Bioorganic & Medicinal Chemistry 8 (2000) 937–943

BIOORGANIC & MEDICINAL CHEMISTRY

Sequence-Selectivity of 5,11-Dimethyl-5*H*-indolo[2,3-*b*]quinoline Binding to DNA. Footprinting and Molecular Modeling Studies

Jarosław Osiadacz,[a,*] Jerzy Majka,[a] Kamil Czarnecki,[b] Wanda Peczyńska-Czoch,[b] Jolanta Zakrzewska-Czerwińska,[a] Łukasz Kaczmarek[c] and W. Andrzej Sokalski[d]

[a]*Ludwik Hirszfeld Institute of Immunology and Experimental Therapy, Polish Academy of Sciences, Weigla 12, 53-114 Wrocław, Poland*

[b]*Institute of Organic Chemistry, Biochemistry and Biotechnology, Wrocław University of Technology, Wybrzeże Wyspiańskiego 27, 50-370 Wrocław, Poland*

[c]*Pharmaceutical Research Institute, Rydygiera 8, 01-783 Warszawa, Poland*

[d]*Institute of Physical and Theoretical Chemistry, Wrocław University of Technology, Wybrzeże Wyspiańskiego 27, 50-370 Wrocław, Poland*

Received 21 June 1999; accepted 1 December 1999

Abstract—Indolo[2,3-*b*]quinolines are a new family of the DNA intercalators showing significant cytotoxic activity. The mechanism of their action is based on the inhibition of DNA topoisomerase II activity. It depends on their ability to induce and stabilize drug–topII–DNA cleavable complexes. Site-specific intercalation of 5,11-dimethyl-5*H*-indolo[2,3-*b*]quinoline (DiMIQ) was analyzed in vitro by DNaseI footprinting and by molecular modeling. To model the DNA–intercalator complex, use was made of the CVFF and ESFF force fields implemented in Insight 97.0 software. Experimental results were verified using a simple statistical model. The DiMIQ molecule was found to bind preferentially to the pBR322 DNA plasmid in the 5′-TGCTAACGC-3′ region between adjacent adenine bases. © 2000 Elsevier Science Ltd. All rights reserved.

Introduction

Numerous recent investigations have been focused on DNA sequence targeting agents. These studies provided insights into the structural and functional features that contribute to the DNA binding selectivity. The discovery of clinically useful anticancer drugs (as well as other DNA-targeting chemotherapeutics) was enabled by several advanced techniques such as footprinting experiments and structural definition via X-ray crystallography, NMR and molecular modeling. These techniques aid better understanding of the DNA–drug interaction and the nature of binding in structural and dynamic terms. DNA-sequence selectivity depends both on the chromophore intercalating moiety and groove-binding properties. There exists evidence that intercalating agents have a DNA sequence-selectivity extending beyond the 2-, 3-bp level.[1] The groove-binding molecules are currently extensively examined. Such compounds usually represent multiple biological activities. The DNA minor-groove-binders have a sequence selectivity of the 10-, 20-bp level.[2] This knowledge permits the design and synthesis of hybrid molecules showing high DNA sequence-selectivity.

In our previous papers we reported the synthesis and SAR studies of indolo[2,3-*b*]quinoline derivatives, which appeared to be a new class of cytotoxic DNA intercalators and topoisomerase II inhibitors.[3–7] We found that the derivatives belonging to the 5*H*- and 6*H*-quinolinium salts series demonstrated significant activity against prokaryotic and eukaryotic organisms, increased the DNA denaturation temperature (ΔT_m in the range 5.2–19 °C) and stimulated the formation of calf thymus topoisomerase II mediated DNA cleavage in the concentration range of 0.6–1.4 μM. We also found that the leading compound 5,11-dimethyl-5*H*-indolo[2,3-*b*]quinoline (DiMIQ) displayed significant activity against Gram-positive bacteria and fungi in the MIC range of 0.03–0.12 μM, was cytotoxic in vitro (ED_{50} values determined against several cancer cell lines ranged from 1.43 to 2.70 μM) and showed significant antitumor properties in vivo, thus prolonging the life span of leukemia P388 and L1210 and melanoma B16 bearing

*Corresponding author. Tel.: +4871-373-22-74 ext. 183; e-mail: osiadacz@immuno.iitd.pan.wroc.pl

0968-0896/00/$ - see front matter © 2000 Elsevier Science Ltd. All rights reserved.
PII: S0968-0896(00)00031-6

animals up to 190, 175 and 240%, respectively.[3,5] According to the McGhee and Von Hippel model,[9] the DNA binding parameters were 0.23×10^6 M^{-1} (for the binding constant K_{app}) and 4.96 (for the number of nucleotides/binding site (n)). We also investigated the electrostatic properties of DiMIQ, which are responsible for the short-range effects resulting from intercalation in a defined geometry (hydrogen bonds, nearest neighbor stacking), and for the long-range stacking effects accounting for the sequence-specific docking of the intercalator into the DNA helix.[7] Long-range electrostatic interactions are responsible for the relative angular orientation of the molecular (DNA–intercalator) complexes, as well as other sequence-dependent DNA properties.[8] This holds not only for hydrogen-bonded systems, but also for sandwich complexes of aromatic molecules.[10–12] We found that the MEP surfaces obtained for DiMIQ and for the other active 5*H*-indolo[2,3-*b*]quinolines formed quite similar patterns.[7] In this case, sequence-selectivity of DNA binding could also be similar in the whole 5*H*-series. Therefore, we decided to perform DNA binding sequence selectivity studies of DiMIQ using both the DNaseI footprinting technique and molecular modeling. In molecular modeling studies we decided to apply a "classical" intercalation model analogous to the computational treatment of a similar 9-hydroxyellipticine structure confirmed by crystallographic data.[13]

Results and Discussion

DNaseI footprinting experiments

To evaluate in detail the interaction between DiMIQ and DNA the DNaseI footprinting was performed. The 385-bp DNA fragment of pBR322 plasmid (Fig. 1) was amplified using a pair of primers $p_{HindIII}$ CW, and p_{BamHI} CCW. After incubation with different amounts of DiMIQ, the DNA was cleaved using DNaseI and separated by denaturing PAGE. Titration of DiMIQ with DNA gave one clear footprint protecting region observed on the 5′-($p_{HindIII}$)-^{32}P-labeled DNA strand (Fig. 2A) and one complementary (but less clear) region on the 5′-(p_{BamHI})-^{32}P-labeled DNA strand (Fig. 2B). The protected region matched the following sequence: 5′-TGCTAACGC-3′.

One-dimensional analysis of the footprinting gel obtained leads to the conclusion that DiMIQ binds sequence-selectively to the DNA duplex and can protect the DNA strand-breaks appearance formation catalyzed by DNaseI. The differential cleavage plot obtained (Fig. 2) shows that, in the absence of DiMIQ, DNaseI can produce an amount of cleavages in the triplex 5′-TAA-3′, which is three times as high as in the presence of 50 μM DiMIQ. The indicated sequence 5′-TAA-3′ occurs in the analyzed fragment 5 times. Further sequence analysis shows that sixth-nucleotide motifs 5′-GCTAAC-3′ and 5′-CTAACG-3′ are not repeated in the investigated fragment (Table 1). Therefore, DNaseI footprinting and sequence analysis allows us to suggest that more than 3 base pairs up- and down-stream should be recognized during the binding process.

Molecular modeling. The structure of the intercalating molecule of 5,11-dimethyl-5*H*-indolo[2,3-*b*]quinoline was obtained in ab initio RHF calculations (LCAO MO SCF using 6-31G basis set), in vacuum, for the basic form of the drug.[7] The DiMIQ structure was then exported to the MSI Insight 97.0 environment. The initial structures of the DNA helix were prepared using Biopolymer and Builder module. Two pentameric fragments of deoxyribonucleic acid were added to the extracted cavity fragment of the DNA backbone. The obtained decameric sequence was similar to the one obtained via footprinting experiments. The choice of a 10-mer was made as a compromise between the following two conflicting requirements: to have a stretch of DNA long enough to be as free of end effects as possible, and to keep the system small enough to be computationally tractable. Similar DNA duplex lengths (up to 12 bp) were used by other investigators.[13]

The starting conformation of the investigated DNA–intercalator complexes was made using the MSI Insight 97.0 software at a Silicon Graphics workstation. Docking was performed in parallel or in perpendicular orientation of the axis of the complementary base-pair and intercalator (Fig. 3). Electrostatic charges and

primer CW: $p_{HindIII}$ *Hind*III site

```
  1  TTCTCATGTT  TGACAGCTTA  TCATCGATAA  GCTTTAATGC  GGTAGTTTAT
 51  CACAGTTAAA  TTGCTAACGC  AGTCAGGCAC  CGTGTATGAA  ATCTAACAAT
101  GCGCTCATCG  TCATCCTCGG  CACCGTCACC  CTGGATGCTG  TAGGCATAGG
151  CTTGGTTATG  CCGGTACTGC  CGGGCCTCTT  GCGGGATATC  GTCCATTCCG
201  ACAGCATCGC  CAGTCACTAT  GGCGTGCTGC  TAGCGCTATA  TGCGTTGATG
251  CAATTTCTAT  GCGCACCCGT  TCTCGGAGCA  CTGTCCGACC  GCTTTGGCCG
301  CCGCCCAGTC  CTGCTCGCTT  CGCTACTTGG  AGCCACTATC  GACTACGCGA
351  TCATGGCGAC  CACACCCGTC  CTGTGGATCC  TCTACGCCGG  ACGCATCGTG
400  GCCGGCATCA  CCGGCGCCAC
```

*Bam*HI site primer CCW: p_{BamHI}

Figure 1. Nucleotide sequence of the investigated 385-bp DNA fragment of pBR322 plasmide. Sequence set up to molecular modeling in solid frame.

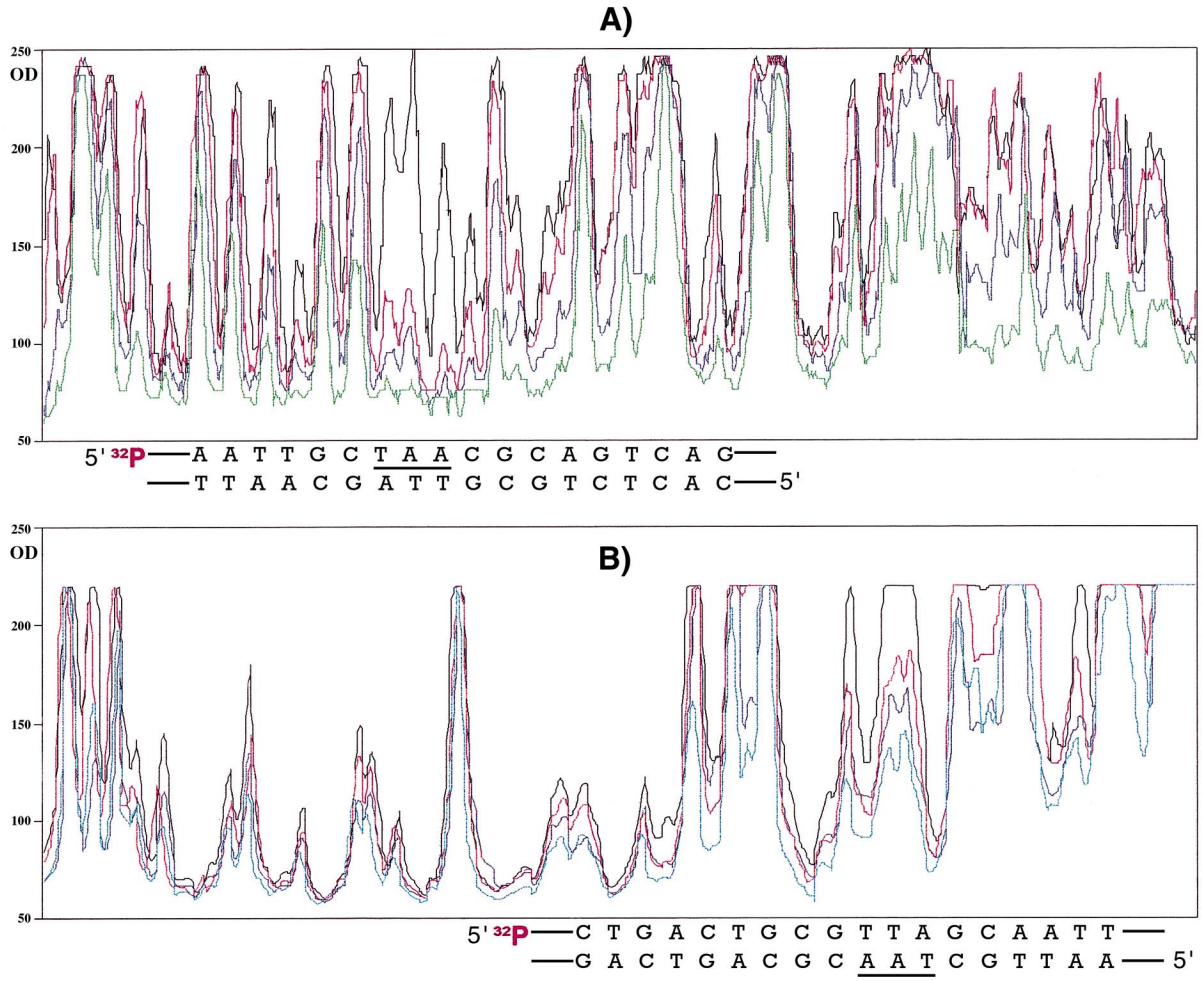

Figure 2. Densitometric scans of the footprinting data. The red, blue and green lines represent the population of cleavages observed in the presence of DiMIQ (5, 25 and 50 μM, respectively) and without DiMIQ — black line. (A) Footprinting on the 5′-($p_{HindIII}$)-^{32}P-labeled strand. The indicated sequence is the same as in Figure 1. (B) Footprinting on the opposite strand 5′-(p_{BamHI})-^{32}P-labeled. The indicated sequence (in 5′ to 3′ manner) is complementary to the sequence listed in Figure 1.

potentials were defined using the ESFF force field. Energy minimizations were performed with the Discover module using the consistent valence force field (CVFF). We made use of the two-force-field hybrid because it was difficult to define correctly the partial charges in the CVFF. The structures of the complexes were optimized to find a minimum on the energy hypersurface of the complex by using the steepest descent algorithm until the derivatives were less than or equal to 0.01 kcal/mol∗A.[2] Two methodologies were applied: (i) optimization of the five different sequences with intercalator in two "canonical" positions (*1* and *1m*), and (ii) optimization of the two intercalating complexes in the preferred sequences 5′-TTGCT-i-AACGC-3′ and 5′-TGCTA-i-ACGCA-3′ in eight different positions (i denotes indolo[2,3-*b*]quinoline molecule inside the DNA cavity). The results are summarized in Tables 2 and 3, respectively and in Figure 4.

Table 1. Frequency of the indicated sequence appearance in the investigated 385-bp DNA fragment of pBR322 plasmid

Sequence	Frequency [digits]
___AA__	10×
__TAA__	5×
___AAC_	2×
__TAAC_	2×
CTAAC	2×
GCTAAC_	1×
_CTAACG	1×

Using a comparatively simple model, we aimed at defining the variation in the DiMIQ–DNA behavior according to the sequence and geometry of the complex. Although the complex energies determined in the ESFF/CVFF are negligible as absolute values, they make it possible to interpret the results in statistical terms (owing to the uniformity of the methods applied, to the similarity of the system (approaching 90%) and to the RMS values obtained), which describe the intercalation complex. The behavioral tendencies defined via this route enable us to select the systems that are optimal terms of both sequence and geometry.

The first optimization set leads to the conclusion that in these two classical orientations (parallel, with nitrogen

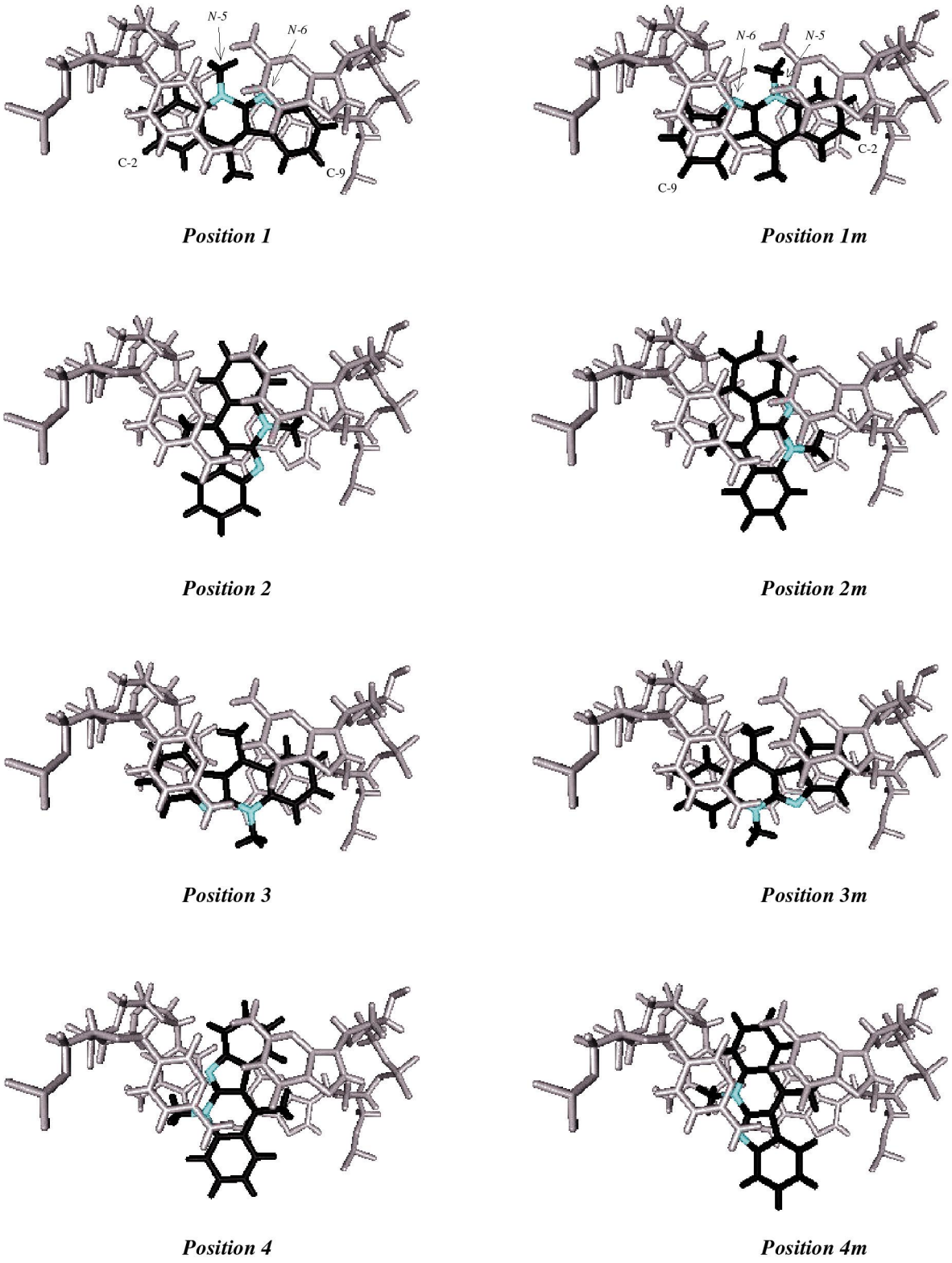

Figure 3. Starting models of the DiMIQ–DNA complex. The 5,11-dimethyl-*5H*-indolo[2,3-*b*]quinoline molecule is shown in black (nitrogen atoms — in blue).

atoms inside the intercalation cavity) the intercalation in the 5′-TGCTA-i-ACGCA-3′ sequence is preferred. The energy values obtained for these orientations vary from −1913.357 to −2096.822 kcal/mol (position *1*) and from −1901.456 to −1978.934 kcal/mol (position *1m*) (Table 2). As clearly shown in Figure 4A and B, the differences in complex energy were significant. According to these results, the 5′-TGCTA-i-ACGCA-3′ sequence can be set as that preferred by DiMIQ in both orientations (*1* and *1m*).

Table 2. Energy minimization of the DNA–DiMIQ intercalation complex in the sequence-dependent manner

Position	Sequence	Total energy		DNA geometry[a]	
		RMS	(kcal/mol)	ψ	ϕ
	ATTGC-i-TAACG[b]	0.00666	−2062.211	−26.76	159.0
	TTGCT-i-AACGC	0.00847	−2096.822	−29.65	169.4
1	TGCTA-i-ACGCA	0.00782	−2068.336	−29.57	174.2
	GCTAA-i-CGCAG	0.00762	−1949.183	−27.81	161.6
	CTAAC-i-GCAGT	0.00940	−1913.357	−29.64	175.0
	ATTGC-i-TAACG	0.00990	−1907.469	−25.73	171.7
	TTGCT-i-AACGC	0.00655	−1925.298	−30.22	173.7
1m	TGCTA-i-ACGCA	0.00811	−1978.934	−27.94	165.5
	GCTAA-i-CGCAG	0.00818	−1946.041	−29.16	170.1
	CTAAC-i-GCAGT	0.01004	−1901.456	−30.95	169.5

[a]Properties of DNA duplex defined as bending angle ψ (angle between helix axes in 1–5 and 6–10 base-pairs), unwinding angle ϕ (angle between base-pair 1 and 10 phosphorus–phosphorus axes).
[b]i — intercalator inside the binding site.

Table 3. Energy minimization of the DNA–DiMIQ intercalation complex in the starting orientation-dependent manner

Sequence	Position	Total energy		DNA geometry[a]	
		RMS	(kcal/mol)	ψ	ϕ
	1	0.00847	−2096.822	−29.65	169.4
	1m	0.00655	−1925.298	−30.22	173.7
	2	0.01097	−1911.411	−28.61	167.6
TTGCT-i-AACGC[b]	*2m*	0.00781	−1925.497	−29.05	168.0
	3	0.01124	−1909.250	−29.82	158.9
	3m	0.00722	−1924.801	−27.55	168.5
	4	0.01008	−1920.656	−28.97	163.8
	4m	0.00870	−1916.842	−29.29	157.0
	1	0.00782	−2068.336	−29.57	174.2
	1m	0.00811	−1978.934	−27.94	165.5
	2	0.01076	−1957.565	−28.74	169.3
TGCTA-i-ACGCA	*2m*	0.00957	−1976.302	−28.21	169.7
	3	0.01124	−1971.871	−28.73	158.0
	3m	0.01008	−1956.689	−29.48	158.8
	4	0.00993	−1967.506	−28.34	159.3
	4m	0.01075	−1953.601	−27.37	153.5

[a]Properties of DNA duplex defined as bending angle ψ (angle between helix axes in 1–5 and 6–10 base-pairs), unwinding angle ϕ (angle between base-pair 1 and 10 phosphorus–phosphorus axes).
[b]i — intercalator inside the binding site.

In the second set we examined eight different positions of the intercalator in both sequences: the most preferred 5′-TGCTA-i-ACGCA-3′ and the neighbor 5′-TTGCT-i-AACGC-3′. The optimized energies were in the range of −1909.250 to −2096.822 kcal/mol for 5′-TTGCT-i-AACGC-3′ and −1953.601 to −2068.336 kcal/mol for 5′-TGCTA-i-ACGCA-3′ (Table 3, Fig. 4C and D). The lowest energy values were obtained in position *1* in both sequences, and the assumption of the ''canonical'' position was achieved (Fig. 5).

In the presence of the intercalating agent some geometrical parameters of the DNA helix become modified. We investigated the influence of DiMIQ intercalation on the unwinding and bending of the DNA. The unwinding angle was defined as the angle between two phosphorus–phosphorus axes, measured between base pairs 1 and 10. Generally, there were no significant differences between the unwinding angles measured in different sequences and the position of intercalation. In every case this angle varied from −25.79 to −30.95°. Additionally, the bending angles (defined as the angle between helix axes of five base-pair sub-domains) were measured. Similarly, there were no significant differences in the DNA helix, the bending angle ranged from 153.5 to 175.0°, in a sequence- and position-independent manner (Tables 2 and 3).

These observations suggest that using the force field method it suffices to investigate the optimal structures of intercalating complexes only in terms of energy minimization. Under such conditions, the geometrical parameters of the helix and intercalator do not depend on the sequence or position of intercalation.

Conclusion

The results of the study allow the following generalizations to be made: (i) The footprinting experiment shows that 5,11-dimethyl-5*H*-indolo[2,3-*b*]quinoline preferentially binds to pBR322 plasmid at one site only. The strongest protection for DNaseI breaking was observed in the 5′-TAA-3′ sequence. (ii) Not only the adjacent base-pairs, but also three or four neighbor base-pairs (up- and downstream) are responsible for the sequence-selectivity of the complex. Only then is it possible to explain the observed specificity of the sequence where protection for the DNaseI breaking occurred. (iii) The molecular modeling approach confirmed the intercalation preference between adjacent adenines. This preference was determined from the lowest calculated values of complex energy (in CVFF/ESFF). (iv) Energy calculations performed for different DiMIQ orientations inside the DNA duplex showed that the most preferred intercalation position (characterized by the lowest complex energy) was the parallel orientation of the long DiMIQ axis and the neighbor base-pair axes (positions *1* and *1m*). (v) No significant correlation between the geometrical properties of the DNA duplex and the sequence or position of intercalation was observed. (vi) Molecular modeling of the optimal complex shows that potential substitution of indolo[2,3-*b*]quinoline core at C-2 and/or C-9 will shift the substitution towards a major helix groove; owing the substituents to groove size, C-2 and C-9 need not be strictly limited (their size and character may be of an arbitrary nature to quite a large extent). (vii) Substitution of indolo[2,3-*b*]quinolines at N-5 or N-6 will shift the substituent to a minor helix groove. Thus the character and size of the substituent will be strictly limited, according to the pattern defined for the fragments of minor-groove binder type. (viii) This simple theoretical model of the indolo[2,3-*b*]quinoline–DNA intercalating complex can be successfully used in more advanced studies, which will hopefully result in a new sequence-specific DNA-targeting agent.[14]

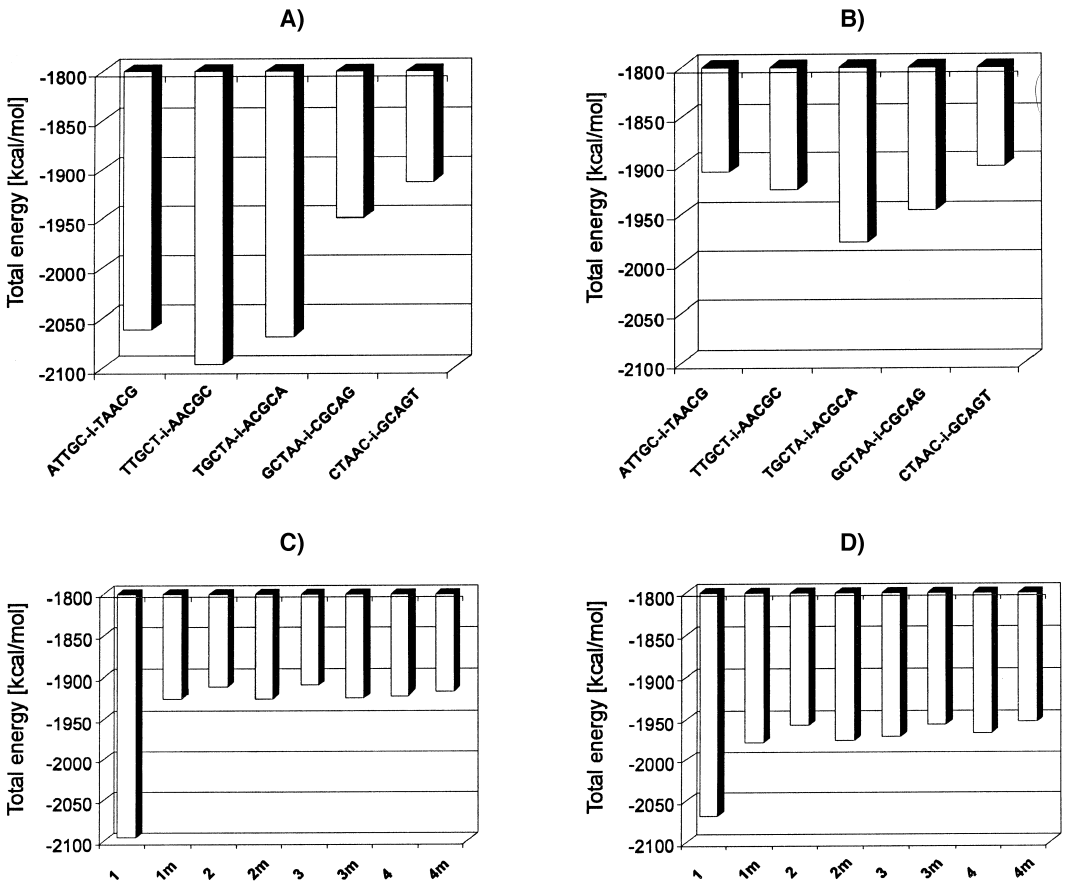

Figure 4. Total energy of the DNA–DiMIQ intercalation complex. (A) In the sequence-dependent manner, for the parallel orientation *1*. (B) In the sequence-dependent manner, for the parallel orientation *1m*. (C) In the starting orientation-dependent manner, for the sequence 5′-TTGCT-i-AACGC. (D) In the starting orientation-dependent manner, for the sequence 5′-TGCTA-i-ACGCA.

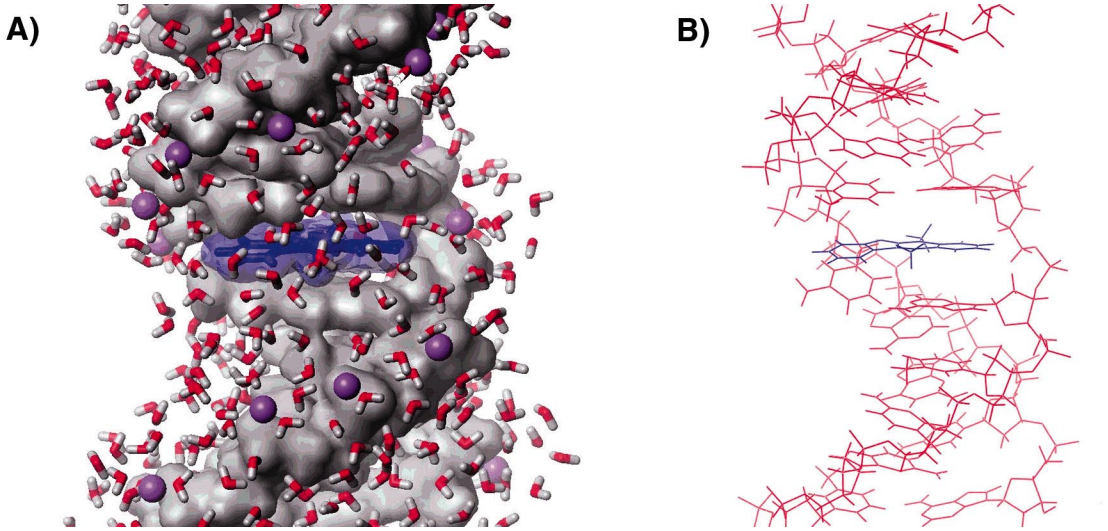

Figure 5. Structure of the most favorable intercalating complex. Sequence TGCTA-i-ACGCA, intercalator in position *1*. (A) Full model of the intercalating complex with Na^+ counterions (violet) and water molecules as well as DNA duplex (presented as Van der Waals surface — gray), and DiMIQ molecule (in stick-style (blue) with transparent Van der Waals surface). (B) Stick model of DiMIQ intercalated into the DNA duplex cavity.

Experimental

Chemicals and biochemicals. Tris base, EDTA, acrylamide, bis-acrylamide tetramethylenediamine and dimethyl sulfate were from Serva. The $p_{HindIII}$ and p_{BamHI} primers and *Bam*HI restriction endonuclease were obtained from Fermantes (Lithuania). Taq polymerase, DNaseI, and tRNA were made by Boehringer-Mannheim. The [γ-^{32}P]-ATP and T4 polynucleotide kinase originated from Amersham-Pharmacia-Biotech as well as sequencing

(dideoxynucleotide-chain-termination method) *Termo Sequenase* kit. X-ray films and other photographic residues were from Kodak. DiMIQ was synthesized at Pharmaceutical Research Institute (Warszawa, Poland) according to an earlier elaborated procedure.[3–5] The remaining chemicals were originated from Polish Chemical Reagents (POCh).

DNaseI footprinting. The 385-bp DNA fragment of pBR322 (Fig. 1) was amplified by PCR using Taq polymerase and a pair of standard primers (one ^{32}P-labeled and one non-labeled): $p_{HindIII}$ clockwise: 5′-GACA GCTTATCATCG-3′, and p_{BamHI} counter-clockwise: 5′-ATGCGTCCGGCGTAGA-3′. The primers were previously 5′-end labeled with [γ-^{32}P]-ATP by T4 polynucleotide kinase.[15] The labeled DNA fragments (10 fmol) were incubated with increasing amounts of DiMIQ (5, 25, 50 μM) in a binding buffer (10 mM Tris–HCl, pH 7.6, 10 mM NaCl, 2 mM $MgCl_2$) at 37 °C for 1 h. The fragments were then subjected to limited DNaseI cleavage as follows: DNA was digested for 2 min with 0.0003 U of DNaseI (added to 50 μL solution containing 10 mM $MgCl_2$ and 5 mM $CaCl_2$). Then the DNaseI cleavage reaction was terminated by addition of 100 μL "Stop solution" (1% SDS, 200 mM NaCl, 20 mM EDTA, pH 8.0, 4 μg/mL tRNA) and by phenol–chloroform extraction. The DNaseI cleavage products were separated on an 8% polyacrylamide–urea-sequencing gel. The sequencing gel was subjected to 1D densitometric analysis using CAM software.[16]

Molecular modeling. All molecular modeling was carried out using Insight 97.0 software.[17] Initial structures of intercalation cavity were prepared using Biopolymer and Builder module, to obtain DNA decamer (according to pBR322 sequence). The geometry of DiMIQ was obtained by quantum-chemical ab initio calculations (LCAO MO SCF using 6-31G basis set), in vacuum, using Gaussian 94 software.[18] Intercalation complexes were prepared by manual docking of the DiMIQ molecule into the prepared DNA decamer. We performed eight models differing from one another in the orientation of DiMIQ in the DNA duplex (Fig. 3). Electrostatic charges and potentials were defined using the ESFF force field. Energy minimizations were performed using the *Discover* module, with the steepest-descent minimization algorithm in vacuum, making use of the CVFF force field. Then the minimizations were repeated for complexes with Na^+ counterions ($Na/P_i = 1$), and 5 Å water layer. Dielectric constants were set to 4. Energy minimizations were performed until the derivatives (RMS) were less than or equal to 0.01 kcal/mol∗Å^2.

Acknowledgements

The research was supported in part by the State Committee for Scientific Research (KBN). We wish to thank the Wrocław Center for Supercomputer and Networking (WCSS Grant No. 10/96) as well as the Molecular Modeling Laboratory (KBN Grant No. 6 P04A 060 09) for providing CPU time dissemination and software.

References

1. Neidle, S.; Jenkins, T. C. In *Methods in Enzymology*; Langone, J. J.; Ed.; Academic Press, 1991, Vol. 203B, p 433.
2. Baraldi, P. G.; Cacciari, B.; Guiotto, A.; Romagnoli, R.; Zaid, A. N.; Spalluto, G. *Il Pharmaco* **1999**, *54*, 15.
3. Kaczmarek, Ł.; Balicki, R.; Nantka-Namirski, P.; Peczyńska-Czoch, W.; Mordarski, M. *Arch. Pharm. (Weinheim)* **1988**, *321*, 463.
4. Pognan, F.; Saucier, J. M.; Paoletti, C.; Kaczmarek, Ł.; Nantka-Namirski, P.; Mordarski, M.; Peczyńska-Czoch, W. *Biochem. Pharmacol*. **1992**, *44*, 2149.
5. Peczyńska-Czoch, W.; Pognan, F.; Kaczmarek, Ł.; Boratyński, J. *J. Med. Chem*. **1994**, *37*, 3503.
6. Kaczmarek, Ł.; Peczyńska-Czoch, W.; Opolski, A.; Wietrzyk, J.; Marcinkowska, E.; Boratyński, J.; Osiadacz, J. *Anticancer Res*. **1998**, *18*, 3133.
7. Kaczmarek, Ł.; Peczyńska-Czoch, W.; Osiadacz, J.; Mordarski, M.; Sokalski, W. A.; Boratynski, J.; Marcinkowska, E.; Glazman-Kusnierczyk, H.; Radzikowski, C. *Bioorg. Med. Chem*. **1999**, *7*, 2457.
8. Liang, G.; Encell, L.; Nelson, M. G.; Switzer, C.; Shuker, D. E. G.; Gold, B. *J. Am. Chem. Soc*. **1995**, *117*, 10135.
9. McGhee, J. D.; Von Hippel, P. H. *J. Mol. Biol*. **1974**, *86*, 469.
10. Naray-Szabo, G.; Ferenczy, G. G. *Chem. Rev*. **1995**, *95*, 829.
11. Price, S. L.; Stone, A. J. *J. Chem. Phys*. **1987**, *86*, 2859.
12. Price, S. L.; LoCelso, F.; Treichel, J. A.; Goodfellow, J. M.; Umrania, Y. *J. Chem. Soc., Faraday Trans*. **1993**, *89*, 3407.
13. Elcock, A. H.; Rodger, A.; Richards, W. G. *Biopolymers* **1996**, *39*, 309.
14. Osiadacz, J.; Zakrzewska-Czerwińska, J.; Czarnecki, K.; Jakimowicz, D.; Peczyńska-Czoch, W.; Kaczmarek, Ł.; Sokalski, W. A. Presented at the *7th International Symposium on Molecular Aspects of Chemotherapy*, Gdańsk, Poland, 9–12 September, 1999.
15. Blaak, H.; Schrempf, H. *Eur. J. Biochem*. **1992**, *229*, 130.
16. Malte J. *CAM* Rev. 2.00 © CYBERTECH Berlin, 1989–1992.
17. Country-Wide License, granted by Polish State Committee for Scientific Research, Insight 97 © Molecular Simulation Inc. 1998–1999.
18. Frish, M. J.; Trucks, G. W.; Schlegel, H. B.; Gill, P. M. W.; Johnson, B. G.; Robb, M. A.; Cheesman, J. R.; Keith, T. A.; Petersson, G. A.; Montgomery, J. A.; Raghavachari, K.; Al.-Laham, M. A.; Zakrzewski, V. G.; Ortiz, J. V.; Foresman, J. B.; Cioslowski, J.; Stefanov, B. B.; Nanayakkara, A.; Challacombe, M.; Peng, C. Y.; Ayala, P. Y.; Chen, W.; Wong, M. W.; Andres, J. L.; Replogle, E. S.; Gomperts, R.; Martin, R. L.; Fox, D. J.; Binkley, J. S.; Defrees, D. J.; Baker, J.; Stewart, J. P.; Head-Gordon, M.; Gonzales, C.; Pople, J. A. *Gaussian 94* Rev. 3.1, © Gaussian Inc., Pittsburgh, PA, 1995.